Virology **296,** 300–307 (2002)
doi:10.1006/viro.2002.1433

Morphology of Marburg Virus NP–RNA

Manos Mavrakis,*[,1] Larissa Kolesnikova,†[,1] Guy Schoehn,*[,‡] Stephan Becker,† and Rob W. H. Ruigrok*[,‡,2]

*EMBL Grenoble Outstation, B.P. 181, 38042 Grenoble Cedex 9, France; †Philipps-Universität Marburg, Institute for Virology, Robert-Koch-Str. 17, Marburg 35037, Germany; and ‡Laboratoire de Virologie Moléculaire et Structurale, EA 2939, Faculté de Médecine de Grenoble, 38700 La Tronche, France

Received October 29, 2001; returned to author for revision December 10, 2001; accepted February 20, 2002

When Marburg virus (MBGV) nucleoprotein (NP) is expressed in insect cells, it binds to cellular RNA and forms NP–RNA complexes such as insect cell-expressed nucleoproteins from other nonsegmented negative-strand RNA viruses. Recombinant MBGV NP–RNA forms loose coils that resemble rabies virus N–RNA. MBGV NP monomers are rods that are spaced along the coil similar to the nucleoprotein monomers of the rabies virus N–RNA. High salt treatment induces tight coiling of the MBGV NP–RNA, again a characteristic observed for other nonsegmented negative-strand virus N–RNAs. Electron microscopy of fixed Marburg virus particles shows that the viral nucleocapsid has a smaller diameter than the free, recombinant NP–RNA. This difference in helical parameters could be caused by the interaction of other viral proteins with the NP–RNA. A similar but opposite phenomenon is observed for rhabdovirus nucleocapsids that are condensed by the viral matrix protein upon which they acquire a larger diameter. Finally, there appears to be an extensive and regular protein scaffold between the viral nucleocapsid and the membrane that seems not to exist in the other negative-strand RNA viruses.

INTRODUCTION

Positive-strand RNA viruses start the infection process after cell entry with the production of viral proteins by using the cellular translation machinery and the viral RNA as messenger. Negative-strand RNA viruses have a viral genome that is in the complementary sense of mRNA. Therefore, the first activity of negative-strand RNA viruses is transcription and production of viral mRNAs. For this purpose, the virions carry an N–RNA structure that consists of the viral RNA (vRNA) that is tightly associated with the viral nucleoprotein (N or NP). At least for influenza virus and vesicular stomatitis virus (VSV) it has been shown that N binds to the sugar-phosphate backbone and that the nucleotide bases are exposed to the outside (Baudin *et al.,* 1994; Iseni *et al.,* 2000). The viral N–RNA has its own RNA-dependent RNA polymerase attached. The polymerase binds either directly to the N–RNA, as is the case for influenza virus, or it binds with the help of a cofactor, such as the phosphoprotein of the paramyxoviruses and the rhabdoviruses (Curran *et al.,* 1994; Horikami and Moyer, 1995; Mellon and Emerson, 1978). The intact N–RNA is the actual template for transcription rather than the naked vRNA and the possible role for the nucleoprotein is exposing the nucleotide bases for efficient reading by the polymerase.

Most of negative-strand RNA viruses have nucleoproteins with a molecular weight of around 60 kDa but the filovirus NP is larger, i.e., 78 kDa according to the sequence for Marburg virus (MBGV) NP (Sanchez *et al.,* 1992). MBGV NP is strongly negatively charged and migrates on an SDS gel with an apparent molecular weight of 92–94 kDa (Becker *et al.,* 1994; Kiley *et al.,* 1988; Sanchez *et al.,* 1992). MBGV NP is strongly phosphorylated at serine and threonine side chains, independent of whether the protein is isolated from virus or from recombinant expression in eukaryotic cells (Becker *et al.,* 1994; Lötfering *et al.,* 1999). The sequences of the Marburg and Ebola virus nucleoproteins are similar for the N-terminal 400 amino acids but highly divergent for the strongly negatively charged C-terminal 300 residues. At the centre of the sequence, there is a region that shows some similarity with the sequences for the nucleoproteins of the rhabdoviruses and even stronger with those of the paramyxoviruses, in particular, respiratory syncytial virus (Sanchez *et al.,* 1992). The MBGV polymerase (L) also binds to the NP–RNA with the help of a cofactor, VP35, which is probably the equivalent of the phosphoprotein of the paramyxo- and rhabdoviruses (Mühlberger *et al.,* 1998). Apart from NP, L, and VP35, the filoviruses are unique in the fact that a fourth protein, VP30, is associated with the nucleocapsid (Becker *et al.,* 1998; Modrof *et al.,* 2001). VP30 is essential for transcription and replica-

[1] These authors contributed equally to this work.

[2] To whom correspondence and reprint requests should be addressed at EMBL Grenoble Outstation, 6 rue Jules Horowitz, 38000 Grenoble, France. Fax: +33-4-76-20-71-99. E-mail: ruigrok@embl-grenoble.fr.

0042-6822/02 $35.00

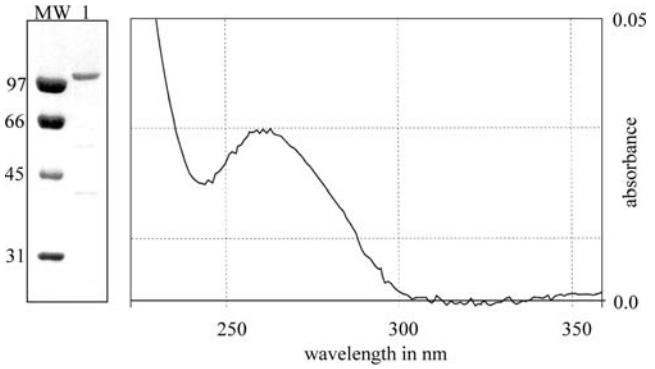

FIG. 1. Characterisation of insect cell-expressed MBGV NP purified by CsCl gradient centrifugation. Left, 10% SDS–PAGE of the visible band in the CsCl gradient, stained with Coomassie blue. MW are molecular weight markers and the lane indicated by 1 contains the NP sample. Right, OD spectrum of the same sample.

tion of an artificial Ebola virus minireplicon but not for a MBGV replicon (Mühlberger *et al.,* 1999).

The nucleoproteins of rabies virus (Iseni *et al.,* 1998; Préhaud *et al.,* 1990) and measles virus (Fooks *et al.,* 1993) have been expressed in insect cells and form N–RNA complexes with cellular RNA that are indistinguishable from actual viral N–RNAs (Iseni *et al.,* 1998; Ravanel *et al.,* 1997; M. Mavrakis, G. Schoehn, and R. W. H. Ruigrok, unpublished results on recombinant measles virus N–RNA). These recombinant N–RNAs can be purified on CsCl gradients on which they migrate to the same density as N–RNA isolated from virus. After the gradient purification, their optical density spectra are characterised by high A260/A280 ratios indicating the presence of nucleic acid (see Results and Discussion). NP of MBGV has also been expressed in insect and mammalian cells and forms nucleocapsid-like structures, although it has not yet been shown if these structures contain RNA (Becker *et al.,* 1994; Kolesnikova *et al.,* 2000).

In this article we describe the morphology of recombinant MBGV NP–RNA imaged by negative-stain electron microscopy (EM). The recombinant NP–RNA coils look somewhat similar to isolated N–RNA from rabies virus. EM of fixed and negatively stained Marburg virus particles showed that the nucleocapsid coil inside virus has a smaller diameter than free, recombinant NP–RNA. This difference in helical parameters could be caused by the presence of other viral proteins in the virion. For the rhabdoviruses it has been shown that the matrix protein condenses the nucleocapsid, resulting in a tightly packed coil with a larger diameter than the free N–RNA coil (Newcomb and Brown, 1981; Schoehn *et al.,* 2001).

RESULTS AND DISCUSSION

MBGV NP was expressed in insect cells that were subsequently opened by freezing/thawing. The cell content was separated over a CsCl gradient that, after spinning, showed a bluish band similar to those observed for the isolation of N–RNA from paramyxo- or rhabdoviruses. This material was dialysed, analysed on SDS–PAGE, and a UV absorption spectrum was taken (Fig. 1). The material contained a major protein component with the migration on SDS–PAGE expected from MBGV NP. The absorption spectrum had an optimum at 260 nm, indicating the presence of nucleic acid. This suggests that recombinant MBGV NP binds to cellular RNA, which has also been shown for insect cell-expressed rabies (rhabdovirus) and measles virus (paramyxovirus) N–RNA (Iseni *et al.,* 1998; M. Mavrakis, G. Schoehn, and R. W. H. Ruigrok, unpublished results). The light bands underneath the strong band for NP in the gel in Fig. 1 are probably degradation products of NP that are still attached to RNA since these bands could not be removed under several salt conditions in additional glycerol gradient centrifugation steps. The A260/A280 ratio of the recombinant MBGV NP–RNA is 1.50 ± 0.02 (four independent samples), higher than that for recombinant measles and rabies virus N–RNAs that contain six and nine nucleotides per N monomer, respectively, but lower than that for influenza virus RNP that has 24 nucleotides per NP (Table 1). However, the direct comparison of these OD ratios is misleading since MBGV NP has a considerably lower molar extinction coefficient than the other N molecules in Table 1. We calculated the nucleotide:NP ratio from OD spectra similar to that in Fig. 1, either directly or in 1% SDS, to denature the NP–RNA and to remove all possible light scattering that may have influenced the OD values. We used an extinction coefficient at 280 nm of 37,550 M^{-1} cm^{-1} (0.485 mg/ml/cm) for denatured NP and of 40,340 M^{-1} cm^{-1} (0.521 mg/ml/cm) for native NP and an extinction coefficient at 260 nm of 12,025 M^{-1} cm^{-1} for RNA nucleotides. The RNA contributes to the signal at 280 nm since the OD260/OD280 for RNA equals 2.0. Therefore, the RNA contributes 50% of its OD260 signal at 280 nm (if the OD260 of the RNA is 1, then the OD280 of the RNA is 0.5). In the same manner,

TABLE 1

A260/A280 Ratios of Negative-Strand Virus N–RNA Complexes

Virus	Sample	A260/A280
Influenza virus (24 nt/NP)	RNP from virus	1.55
	Purified NP from virus	0.59
	Naked RNA from virus	1.80
Rabies virus (9 nt/N)	N–RNA from virus	1.22
	N–RNA recombinant	1.24
Measles virus (6 nt/N)	N–RNA recombinant	1.17
Marburg virus (12 or 15 nt/NP)	N–RNA recombinant	1.50

Note. The A260/A280 ratios for influenza and rabies virus components were published before (Ruigrok and Baudin, 1995; Iseni *et al.,* 1998).

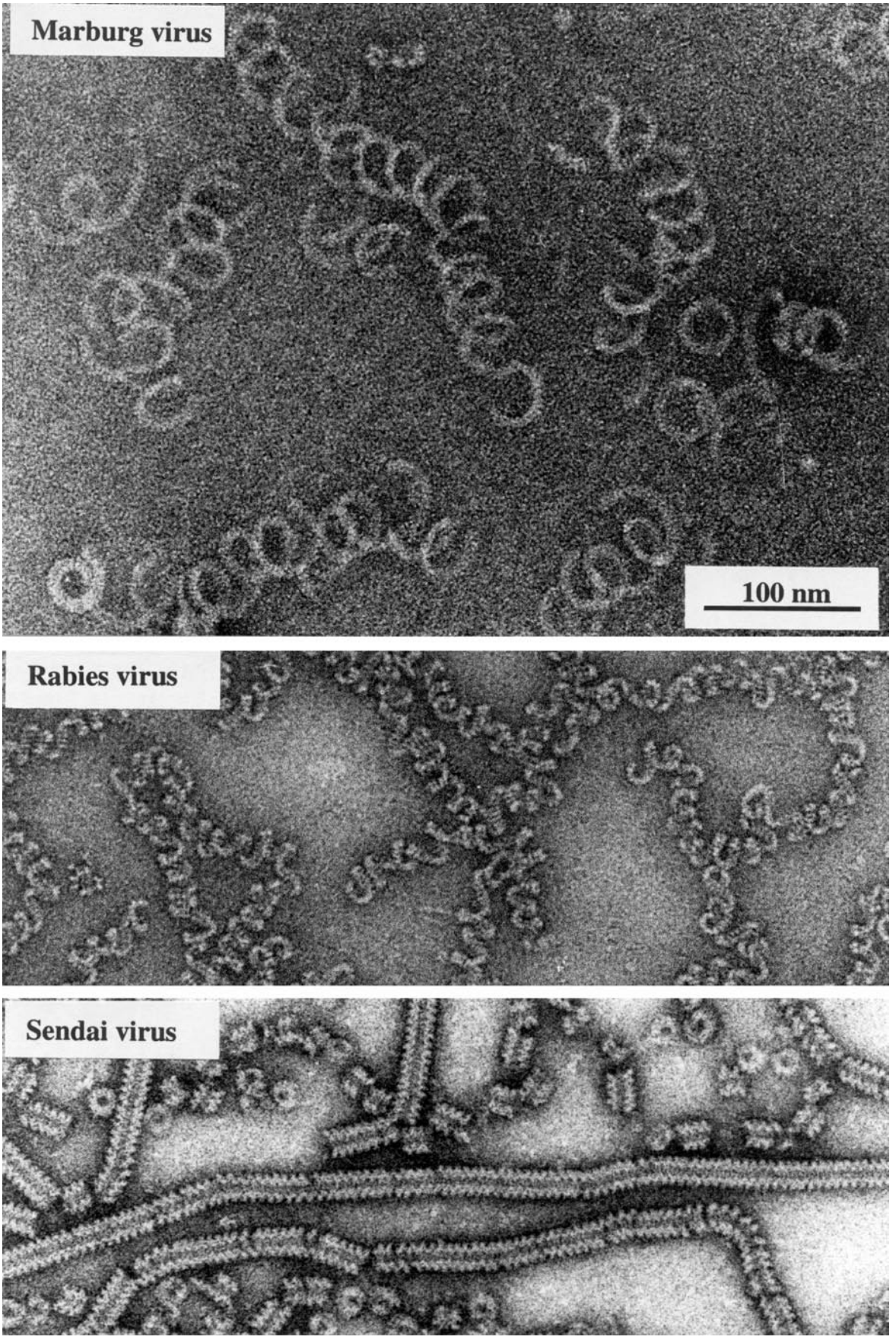
Marburg virus
100 nm
Rabies virus
Sendai virus

TABLE 2

Measurements on Recombinant Marburg Virus NP-RNA and Virus Particles

Stain/cryo	NP–NP spacing	Height	Length
	Dimensions of NP monomers in coils and rings		
SST	3.4 ± 0.3 nm (n = 44)	5.2 ± 0.5 nm (n = 13)	10.4 ± 1.3 nm (n = 19)
Uranyl acetate	3.6 ± 0.4 nm (n = 48)		
Cryo	3.5 ± 0.5 nm (n = 15)		
	Pitch	Outer diameter	Inner diameter
	Measurements on coils (uranyl acetate only)		
Tight coils	8.7 ± 0.6 nm (n = 22)	38.5 ± 1.4 nm (n = 28)	20.1 ± 2.1 nm (n = 26)
Loose coils		40.6 ± 2.6 nm (n = 30)	25.0 ± 2.2 nm (n = 14)
Width virus	Spacing central coil	Outer diameter central coil	Spacing of rods at membrane
	Features from fixed, negatively stained virus particles		
71.5 ± 3 (n = 25)	6.0 ± 0.4 nm (n = 26)	27 ± 1 nm (n = 25)	4.6 ± 0.4 nm (n = 25)

Note. The values for the measurements are given as average plus or minus the standard error of the population with the number of measurements in parentheses.

the protein also contributes at 260 nm since the OD260/OD280 of pure protein is 0.57. Taking these contributions into account and using the extinction coefficients given above, we calculated an nt:NP ratio of 15.2 from the native sample in Fig. 1 and of 11.7 of the same sample in 1% SDS. From another SDS denatured sample we calculated a ratio of 13.0. Since all other negative-strand RNA viruses have nt:NP ratios that are multiples of 3, it is possible that each MBGV NP monomer binds 12 or 15 nucleotides.

Figure 2 shows the recombinant MBGV NP–RNA coils after negative staining with uranyl acetate in comparison with negatively stained N–RNAs of a rhabdovirus (rabies virus) and a paramyxovirus (Sendai virus) (both these N–RNAs were isolated from virus). All three structures form helical coils but differ in the tightness and diameters of the coils. The outer diameter of the MBGV NP–RNA coils is about 40 nm (Table 2), compared with 22 nm for the rabies virus (Iseni *et al.,* 1998) and 20 ± 1 nm (30 measurements) for the Sendai virus coils. In the samples of recombinant MBGV NP–RNA we did not find the small N–RNA rings with about 10 N monomers per ring that were found in a recombinant rabies virus N–RNA preparation (Iseni *et al.,* 1998; Schoehn *et al.,* 2001). This could mean that MBGV NP does not bind to short cellular RNAs such as tRNAs. It is interesting to note that the lower the amount of nucleotides bound per nucleoprotein monomer, the tighter the coil.

In some images one can see the NP monomers that make up the coils (Fig. 3a). These monomers consist of rods that are spaced every 3.5 nm along the coil (Table 2), which is the same as the spacing of the rabies virus N monomers (Iseni *et al.,* 1998; Schoehn *et al.,* 2001). Since the MBGV NP–RNA coils turn in space, the monomers are sometimes seen lying lengthwise on the carbon support film and sometimes end-on. The negative stain will mainly outline that part of the monomers that is in direct contact with the carbon support film. We will define the length of the monomers as the maximum width of the coil, the width of the monomers as the spacing along the coil (~3.5 nm), and the height of the monomers as the distance in the third dimension that can be derived from the minimum width of the coil. The height of the monomers was thus deduced to be 5.2 nm (Table 2), which is also the same as the height of rabies virus N. The measurements on the maximum diameter of the coils, corresponding to the length of NP, were very variable leading to a high standard deviation compared to those for the spacing and the height. This could be due to a flexible part or domain of the protein that sometimes contributes to its length and sometimes not. The average value for the length of NP was 10.4 nm but the highest value was 12.6 nm. Rabies virus N is only 9.4 nm long (Schoehn *et al.,* 2001). The same kind of coils were observed in cryo-EM of MBGV NP–RNA (not shown), suggesting that the coils observed after nega-

FIG. 2. Electron micrographs of negatively stained nucleoprotein–RNA complexes of nonsegmented negative-strand RNA viruses. The MBGV sample is recombinant NP–RNA produced in insect cells and subsequently negatively stained for EM with 1% uranyl acetate. The rabies and Sendai samples are N–RNA isolated from virus and purified over a CsCl gradient and subsequently negatively stained for EM with 1% sodium silicotungstate. The magnification of the three panels is the same and indicated by the bar in the top picture.

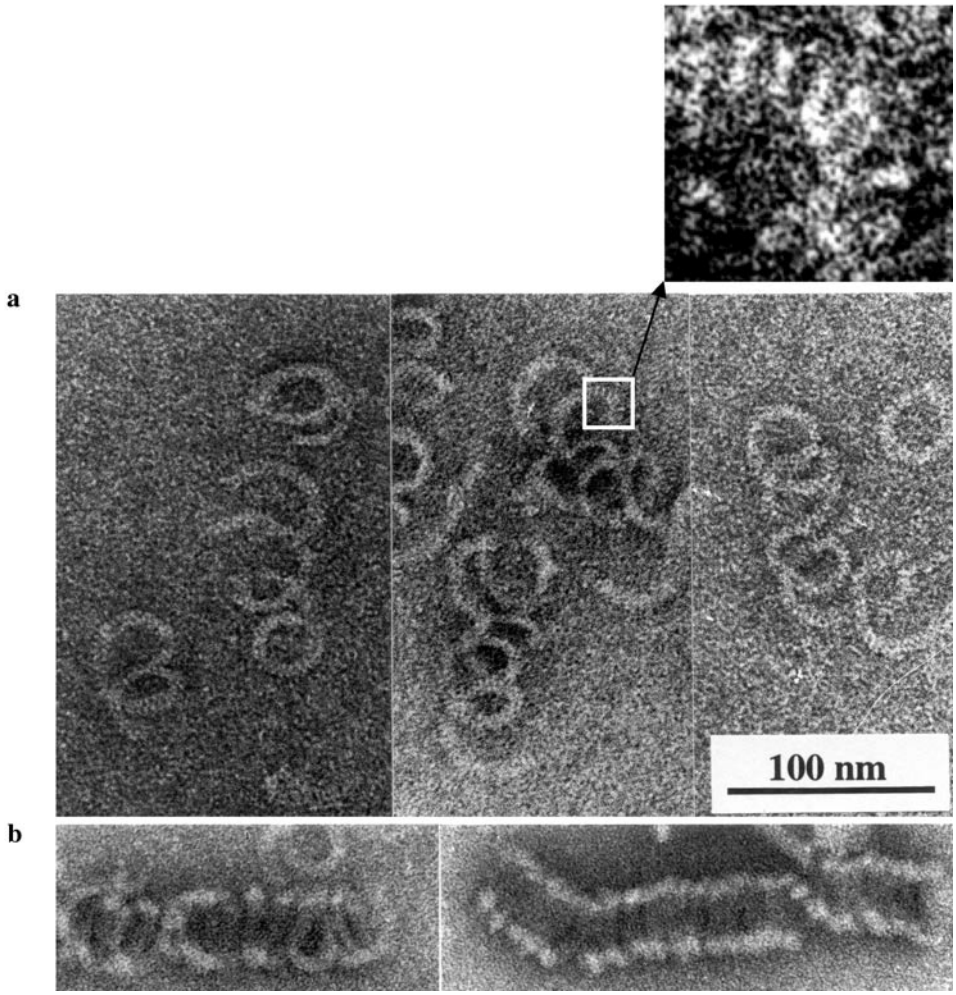

FIG. 3. Morphology of MBGV NP monomers and coils in high salt. (a) Recombinant NP–RNA negatively stained with 1% uranyl acetate. At several places the NP monomers making up the coils are visible. The white rectangle and the arrow point to a magnification of this area where the monomers are particularly well resolved. (b) Recombinant MBGV NP–RNA was dialysed toward 1 M NaCl and negatively stained with 1% uranyl acetate. The resolution in these images is lower than in (a) because of the high electron dose that was used in combination with the high salt concentration. (a) and (b) have the same magnification, as indicated by the bar in (a).

tive staining are close to the shape of the actual sample in solution. The NP–NP spacing measured from the cryomicrographs was the same as that measured from negatively stained coils (Table 2).

Subsequently, recombinant MBGV NP–RNA was dialysed to 1 M NaCl before negative staining (Fig. 3b). Here we observed tight coils with a similar outer diameter as the loose coils in Figs. 2 and 3a (Table 2). The pitch of the coils is larger than the height of the NP monomers but smaller than their average length. Therefore the orientation of the monomers in the tight coils is not clear. This salt-dependent tight coiling behaviour has also been observed for paramyxo- and rhabdovirus nucleocapsids (Heggeness *et al.,* 1980) and is possibly due to the neutralisation of a strongly charged domain on NP by the salt. In short, recombinant MBGV NP–RNA and the NP monomers resemble in many aspects those of rabies virus and the salt-dependent coiling of the NP–RNA is also similar to that of the other nonsegmented negative-strand RNA viruses.

Figure 4 shows negatively stained, fixed, intact Marburg virus. Although the virions seem to have some disorders in the envelope that are probably caused by the fixation step with formaldehyde, the virus particles were found to be very regular with a well-defined diameter (Table 2 and schematic model in Fig. 5). One can observe an internal structure that is most likely made up by the nucleocapsid with an outer diameter of 27 nm and a lengthwise repeat (probably the pitch of the coil) of 6 nm. Close to and perpendicular to the membrane, one observes a striation with a repeat of 4.6 nm. It seems as if the nucleocapsid is tightly scaffolded into the middle of the virion. The repeat (pitch) of the nucleocapsid inside the virus is close to that of the high-salt, tightly coiled recombinant material. The main difference between the recombinant NP–RNA and the viral nucleocapsids

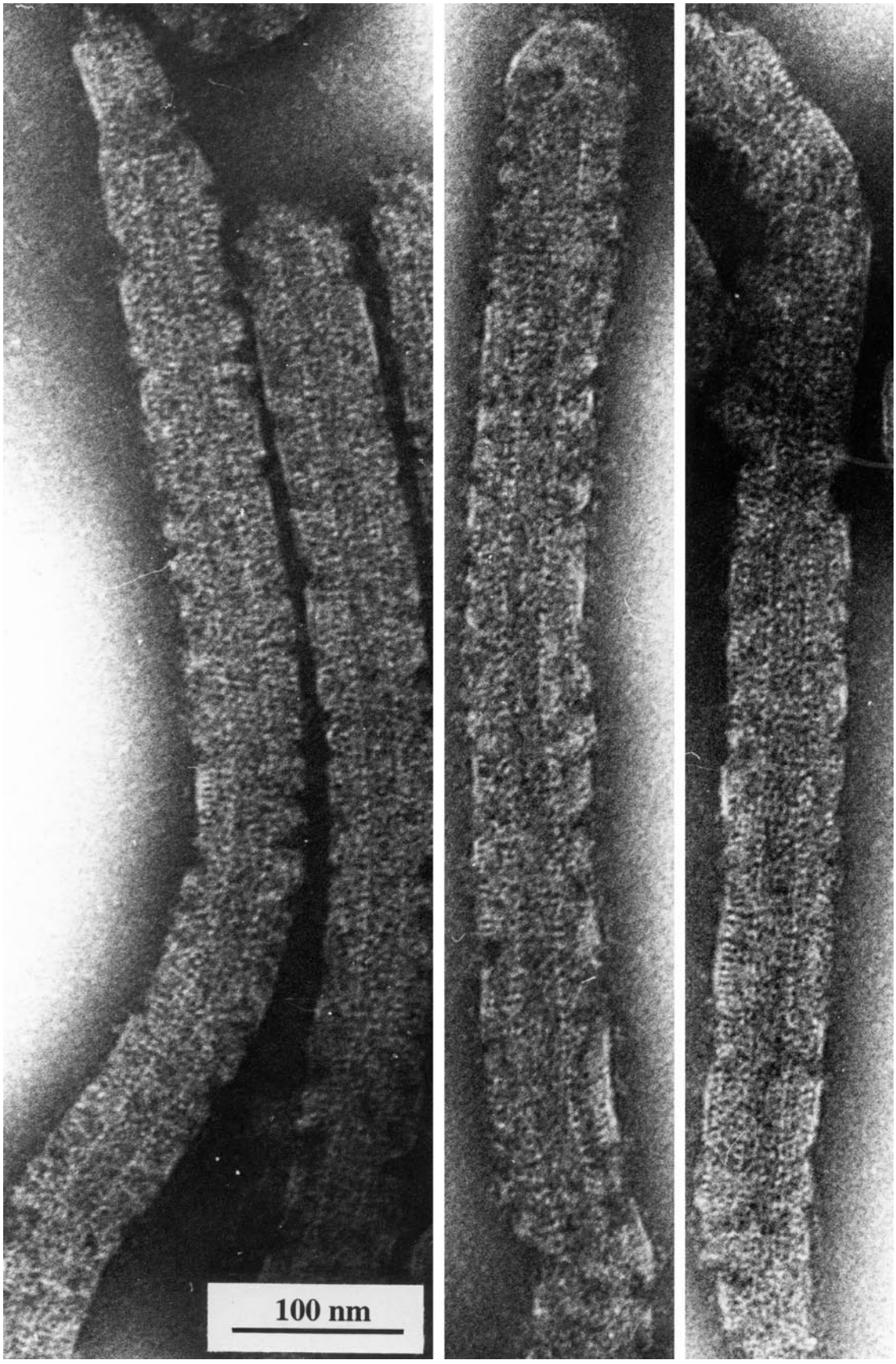

FIG. 4. Electron micrographs of Marburg virus fixed with 4% formaldehyde and negatively stained with 2% phophotungstic acid.

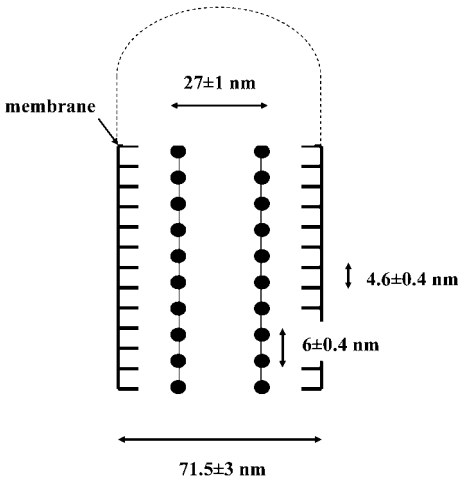

FIG. 5. Schematic model of the negatively stained virus as shown in Fig. 4, indicating the structural features described in the text plus the various measurements of spacings and diameters. The numbers of measurements are given in Table 2.

seems to be the width of the nucleocapsid coil. It is possible that the other viral proteins that are associated with the viral nucleocapsids have an influence on the helical parameters. It is known for the rhabdoviruses that the diameter of the nucleocapsid coil of CsCl purified, viral N–RNA is the same as that for recombinant N–RNA but different from that of the nucleocapsid inside the virus (Schoehn *et al.,* 2001). For this group of viruses, the differences between free and viral nucleocapsids in coiling parameters and tilt angles of the N monomers relative to the coil axis are induced by the viral matrix protein that condenses the nucleocapsid into the form it has inside the intact virus (Newcomb and Brown, 1981; Newcomb *et al.,* 1982). Modification of the helical parameters of the nucleocapsid by other viral proteins would be a characteristic shared between rhabdo- and filoviruses. It is interesting to note that MBGV nucleocapsids inside infected cells are already highly organised and have the same diameter as the nucleocapsid in the virus measured here (Kolesnikova *et al.,* 2000). This also seems to be the case for the rhabdoviruses where the matrix protein first condenses the nucleocapsid before it goes into the virion (Odenwald *et al.,* 1986). It would seem that, both for filo- and for rhabdoviruses, it is the preformed intracellular nucleocapsid that determines the shape of the virus particle. This does not seem to be the case for the ortho- and paramyxoviruses where particle shape may be determined by the interaction of the matrix protein and the viral membrane with its embedded spikes and lipid rafts.

Finally, the negatively stained images of MBGV presented here confirm previous micrographs of thin-sectioned infected cells, such as shown by Feldmann and Klenk (1996), that the virus has a very regular structure but add the observation of an extensive and regular protein network between the membrane and the nucleocapsid that may be made up by VP40 and VP24, the two filovirus matrix proteins.

MATERIALS AND METHODS

Expression and purification of recombinant Marburg virus NP–RNA

Recombinant AcNPV (*Autographa californica* nuclear polyhedrosis virus; strain vVL-NP) coding for full-length MBGV NP (Lötfering *et al.,* 1999) was used to infect *Sf21* insect cells at a multiplicity of infection (m.o.i.) of 5. Insect cells were grown in TC100 medium supplemented with 10% foetal calf serum and antibiotics in monolayer cultures at 27°C. Six 175-cm^2 flasks were infected and the cells harvested at 48 h postinfection. The cells were pelleted at 350 *g* for 10 min and resuspended in a hypotonic buffer solution (20 mM Tris–HCl pH 8, 50 mM NaCl, 1 mM EDTA) in the presence of protease inhibitor (Complete-EDTA free, Roche Diagnostics). Cells were lysed by three cycles of freezing and thawing and the cell debris pelleted at 12,000 *g* and 4°C for 15 min. The cleared lysate was then loaded on top of a continuous 20–40% w/w CsCl gradient in 20 mM Tris–HCl pH 8, 200 mM NaCl and centrifuged at 30,000 rpm and 12°C for 16 h in a SW41 rotor (Beckman; 110,000 *g*). The visible band in the gradient, corresponding to the recombinant NP–RNA, was collected by puncturing the tube and the presence of the nucleoprotein was verified by 10% SDS–PAGE. The CsCl was dialysed away in 100 mM NaCl, 20 mM Tris–HCl pH 8, and the sample was checked for the presence of RNA by taking a UV absorption spectrum.

Marburg virus particles

All work with infectious MBGV was performed under BSL-4 conditions. For analysis of cell-free virions, approximately 10^7 Vero cells were infected with MBGV (strain Musoke) at an m.o.i. of 1 plaque forming unit (PFU) per cell. Culture medium was harvested at 5 days postinfection and virions were purified by centrifugation through a 20% sucrose cushion. The pellet was resuspended in PBS containing 4% paraformaldehyde and incubated for 24 h.

Electron microscopy

A drop of the fixed MBGV suspension was deposited on a Formvar/carbon-coated nickel grid for 1 min, washed with PBS, and negatively stained with 2% phosphotungstic acid. The samples were studied with a JEOL 1200 EXII microscope at 40,000× magnification, calibrated with negatively stained crystals of catalase.

The recombinant NP–RNA was either directly prepared for negative staining or first dialyzed to 1 M NaCl in 20 mM Tris–HCl pH 8. Samples were first incubated for 10 min at 37°C and then absorbed to carbon support film and negatively stained with 1% uranyl acetate. The

low salt samples were studied under low-dose conditions in the JEOL microscope but the high salt samples under high-dose conditions since the density of particles on the carbon film was too low. Alternatively, the low salt samples were prepared for cryo-EM and observed with a Philips CM20 LaB6 microscope at 38,000× magnification as described before (Schoehn *et al.,* 2001).

ACKNOWLEDGMENTS

This work was financed by the EMBL and the Deutsche Forschungsgemeinschaft, Sonderforschungsbereich 286, TP A6 and 535, TP B9. We thank Drs. Winfried Weissenhorn and Florence Baudin (EMBL-Grenoble) for many fruitful discussions.

REFERENCES

Baudin, F., Bach, C., Cusack, S., and Ruigrok, R. W. H. (1994). Structure of influenza virus RNP. I. Influenza virus nucleoprotein melts secondary structure in panhandle RNA and exposes the bases to the solvent. *EMBO J.* **13,** 3158–3165.

Becker, S., Huppertz, S., Klenk, H.-D., and Feldmann, H. (1994). The nucleoprotein of Marburg virus is phosphorylated. *J. Gen. Virol.* **75,** 809–818.

Becker, S., Rinne, C., Hofsäβ, U., Klenk, H.-D., and Mühlberger, E. (1998). Interactions of Marburg virus nucleocapsid proteins. *Virology* **249,** 406–417.

Curran, J., Pelet, T., and Kolakofsky, D. (1994). An acidic activation-like domain of the Sendai virus P protein is required for RNA synthesis and encapsidation. *Virology* **202,** 875–884.

Feldmann, H, and Klenk, H.-D. (1996). Marburg and Ebola viruses. *Adv. Vir. Res.* **47,** 1–52.

Fooks, A. R., Stephenson, J. R., Warnes, A., Dowset, A. B., Rima, B. K., and Wilkinson, G. W. G. (1993). Measles virus nucleocapsid protein expressed in insect cells assembles into nucleocapsid-like structures. *J. Gen. Virol.* **74,** 1439–1444.

Heggeness, M. H., Scheid, A., and Choppin, P. W. (1980). Conformation of the helical nucleocapsids of paramyxoviruses and vesicular stomatitis virus: Reversible coiling and uncoiling induced by changes in salt concentration. *Proc. Natl. Acad. Sci. USA* **77,** 2631–2635.

Horikami, S. M., and Moyer, S. A. (1995). Alternative amino acids at a single site in the Sendai virus L protein produce multiple defects in RNA synthesis in vitro. *Virology* **211,** 577–582.

Iseni, F., Barge, A., Baudin, F., Blondel, D., and Ruigrok, R. W. H. (1998). Characterization of rabies virus nucleocapsids and recombinant nucleocapsid-like structures. *J. Gen Virol.* **79,** 2909–2919.

Iseni, F., Baudin, F., Blondel, D., and Ruigrok, R. W. H. (2000). Structure of the RNA inside the vesicular stomatitis virus nucleocapsid. *RNA* **6,** 270–281.

Kiley, M. P., Cox, N. J., Elliott, L. H., Sanchez, A., DeFries, R., Buchmeier, M. J., Richman, D. D., and McCormick, J. B. (1988). Physicochemical properties of Marburg virus: Evidence for three distinct strains and their relationship to Ebola virus. *J. Gen. Virol.* **69,** 1957–1967.

Kolesnikova, L., Mühlberger, E., Ryabchikova, E., and Becker, S. (2000). Ultrastructural organization of recombinant Marburg virus nucleoprotein: Comparison with Marburg virus inclusions. *J. Virol.* **74,** 3899–3904.

Lötfering, B., Mühlberger, E., Tamura, T., Klenk, H.-D., and Becker, S. (1999). The nucleoprotein of Marburg virus is target for multiple cellular kinases. *Virology* **255,** 50–62.

Mellon, M. G., and Emerson, S. U. (1978). Rebinding of transcriptase components (L and NS proteins) to the nucleocapsid template of vesicular stomatitis virus. *J Virol* **27,** 560–567.

Modrof, J., Möritz, C., Kolesnikova, L., Konakova, T., Hartlieb, B., Randolf, A., Mühlberger, E., and Becker, S. (2001). Phosphorylation of Marburg virus VP30 at serines 40 and 42 is critical for its interaction with NP inclusions. *Virology* **287,** 171–182.

Mühlberger, E., Lötfering, B., Klenk, H.-D., and Becker, S. (1998). Three of the four nucleocapsid proteins of Marburg virus, NP, VP35, and L, are sufficient to mediate replication and transcription of Marburg virus-specific monocistronic minigenomes. *J. Virol.* **72,** 8756–8764.

Mühlberger, E., Weik, M., Volchkov, V. E., Klenk, H.-D., and Becker, S. (1999). Comparison of the transcription and replication strategies of Marburg virus and Ebola virus by using artificial replication systems. *J. Virol.* **73,** 2333–2342.

Newcomb, W. W., and Brown, J. C. (1981). Role of the vesicular stomatitis virus matrix protein in maintaining the viral nucleocapsid in the condensed form found in native virions. *J. Virol.* **39,** 295–299.

Newcomb, W. W., Tobin, G. J., McGowan, J. J., and Brown, J. C. (1982). *In vitro* reassembly of vesicular stomatitis virus skeletons. *J. Virol.* **41,** 1055–1062.

Odenwald, W. F., Arnheiter, H., Dubois-Dalcq, M., and Lazzarini, R. A. (1986). Stereo images of vesicular stomatitis virus assembly. *J. Virol.* **57,** 922–932.

Préhaud, C., Harris, R. D., Fulop, V., Koh, C. L., Wong, J., Flamand, A., and Bishop, D. H. (1990). Expression, characterization, and purification of a phosphorylated rabies nucleoprotein synthesized in insect cells by baculovirus vectors. *Virology* **178,** 486–497.

Ravanel, K., Castelle, C., Defrance, T., Wild, T. F., Charron, D., Lotteau, V., and Rabourdin-Combe, C. (1997). Measles virus nucleocapsid protein binds to FcgammaRII and inhibits human B cell antibody production. *J. Exp. Med.* **186,** 269–278.

Ruigrok, R. W. H., and Baudin, F. (1995). Structure of influenza virus ribonucleoprotein particles. II. Purified RNA-free influenza virus nucleoprotein forms structures that are indistinguishable from the intact influenza virus ribonucleoprotein particles. *J. Gen. Virol.* **76,** 1009–1014.

Sanchez, A., Kiley, M. P., Klenk, H.-D., and Feldmann, H. (1992). Sequence analysis of the Marburg virus nucleoprotein gene: Comparison to Ebola virus and the other non-segmented negative-strand RNA viruses. *J. Gen. Virol.* **73,** 347–357.

Schoehn, G., Iseni, F., Mavrakis, M., Blondel, D., and Ruigrok, R. W. H. (2001). Structure of recombinant rabies virus N-RNA and identification of the phosphoprotein binding site. *J. Virol.* **75,** 490–498.